



Short Communication

Sub-micrometer precision of optical imaging to locate the free surface of a micrometer fluid shape

J.M. Montanero^a, E.J. Vega^a, C. Ferrera^{b,*}^a Department of Mechanical, Energetic and Material Engineering, University of Extremadura, Avda. De Elvas s/n, E-06071 Badajoz, Spain^b Department of Aerospace Engineering and Fluid Mechanics, University of Seville, Camino de los Descubrimientos s/n, E-41092 Sevilla, Spain

ARTICLE INFO

Article history:

Received 6 April 2009

Accepted 21 July 2009

Available online 28 July 2009

Keywords:

Free surface

Image analysis

Optical imaging

Liquid film

ABSTRACT

In this note, we explore the precision of the optical imaging method for measuring the free surface position of a micrometer fluid shape. For this purpose, images of a liquid film deposited on a rod were acquired and processed. The resulting contour was compared with the corresponding solution to the Young-Laplace equation. The average deviation was about 30 nm, 25 times smaller than the pixel size, reflecting the validity of optical imaging for most applications in microfluidics.

© 2009 Elsevier Inc. All rights reserved.

1. Introduction

The controllable production of micrometer flowing particles has been extensively studied in recent years because of its relevance for a broad field of practical and industrial applications [1]. A coherent understanding of micro- and nano-scale particle producing interfacial flows is essential for a rational design and manufacturing strategy. In this context, optical imaging may provide useful information to characterize flow transitions or breakage processes [2–7]. There is, however, a limitation inherent in the optical imaging method that constitutes a serious obstacle in this context: the images become more blurred as the object's size decreases due to diffraction, independently of the quality of the focus. A natural question is whether image processing techniques can overcome that limitation and still provide reliable results for very small fluid configurations. Although the use of optical imaging in microfluidics has increased sharply in recent years [6], this question has yet to be properly answered. In this context, Sattler et al. [7] have claimed that they were able to resolve free surface perturbations down to an amplitude of 80 nm, which corresponds to significant superresolution. In this work, we examine the precision of optical imaging to locate the free surface of a micrometer fluid configuration. For this purpose, the contour of an axisymmetric liquid film deposited on a rod was measured and compared with the corresponding (exact) solution to the Young-Laplace equation. The present paper builds on our earlier study of micrometer deformations of milli-

metric liquid bridges [8] and improves the resolution achieved by an order of magnitude.

2. Experimental method

Fig. 1 shows the apparatus used in our experiments. A liquid film of hexadecane was deposited on a rod (A) placed vertically through a triaxial orientation system (B). The rod was made of tungsten carbide, $100 \pm 0.3 \mu\text{m}$ in diameter, and with a cylindricity tolerance below $0.2 \mu\text{m}$. This last feature determined the choice of this component material. Liquid was fed by a stepper motor through a steel capillary (C) $150 \mu\text{m}$ in internal diameter. The capillary was aligned with the rod at a distance of about $50 \mu\text{m}$ by using a triaxial translation stage (D). A droplet hanging from the capillary was collected by the rod. Because of the very small size of the droplet, gravity did not detach it from the capillary. Instead, we used the drag force exerted by the draught coming from a glass tube (E), 1.15 mm in internal diameter, and coaxial with the feeder capillary. This force also allowed us to control the film position on the rod. Digital images of 800×800 pixels were acquired using a JAI TM-1405GE CCD camera (F) equipped with optical lens (Goyo Optical Inc. objective HR 2/3" F2.8/50 mm, zoom $2\times$, and extending rings 160 mm in length) (G) providing a frame covering an area of about $575 \times 575 \mu\text{m}$. The magnification obtained was $0.720 \mu\text{m}/\text{pixel}$. The camera could be displaced by means of a triaxial translation stage (H) to focus on the liquid film. The fluid configuration was illuminated by backlighting (I). All the components of the experimental apparatus were mounted on an optical table with a pneumatic anti-vibration isolation system (J) to damp the vibrations coming from the building.

* Corresponding author. Fax: +34 954486041.

E-mail addresses: jmm@unex.es (J.M. Montanero), ejvega@unex.es (E.J. Vega), cfl@us.es, conradofll@gmail.com (C. Ferrera).

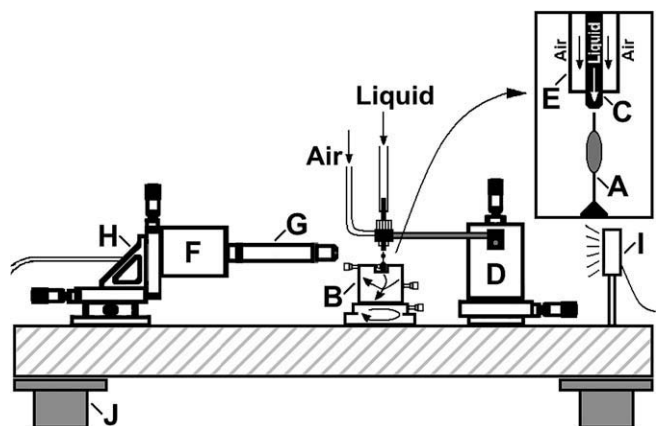


Fig. 1. Experimental apparatus: supporting rod (A), triaxial orientation system (B), steel capillary (C), triaxial translation stage (D), glass tube (E), CCD camera (F), optical lens (G), triaxial translation stage (H), backlighting (I), and anti-vibration isolation system (J).

Images of a calibration grid were acquired with less magnification lenses, and subsequently processed to verify that the pixel aspect ratio was practically unity. It must be noted that, as will be shown in Section 3, the discrepancies between the detected edges and their expected shapes were of the order of tens of nanometers. We know no calibration element from whose analysis one can evaluate an optical distortion of that magnitude. Therefore, the optical distortion of the lenses used in the experiments was not evaluated. The magnification of the image acquisition system was determined before conducting each experiment. For this purpose, images of the rod were acquired with working distances within an interval of about $150\ \mu\text{m}$, for which the focus was suitable and qualitatively the same. Each image's focus was evaluated quantitatively by calculating the width of the edges from the gray intensity matrix. The selected working distance was that yielding the minimum value of the edge width, i.e., the optimum focus. The image acquired with the optimum focus was used to calculate the magnification.

Once the working distance was fixed, the experiment was performed. A micrometer droplet was formed at the exit of the feeder capillary and detached from it by the draught coming from the glass tube. The liquid was collected by the rod, so that a film spread over its surface. The liquid film descended slowly onto the rod until the draught was halted. Then, we waited for several minutes until the migration of the liquid was completed and the film remained in equilibrium (Fig. 2). We verified that the evaporation of the film

was significant only over a time scale of hours. It is worth mentioning that this experimental technique allows one to study the effect of very small filament diameters on the advancing contact angle, and consequently on the wetting hysteresis.

Ten images of the liquid film at equilibrium were acquired and processed. Here, we shall briefly describe the main aspects of the image processing technique. Details of the procedure can be found elsewhere [8]. The contours of the supporting rod and the free surface in the image were detected using a two-stage procedure. In the first stage, a set of pixels probably corresponding to the contour being sought was extracted using Canny's method. The accuracy of Canny's method is limited to the pixel size. In the second stage, the accuracy of the detected contours was improved to the sub-pixel level by analyzing the gray intensity profile along the direction ξ normal to the contour. Fitting the sigmoid (Boltzmann) function [9] to the gray intensity values allowed us to obtain a continuous function in the transient region of the gray profile (Fig. 2). The contour point was found by applying the local thresholding criterion. The number of resulting contour points was approximately equal to the number of pixels of the image along the vertical direction.

Once the contours had been detected, they were rotated to their vertical position (the rotation angle was less than 0.2° in all the cases analyzed), and the symmetry axis $x_s(z)$ was found. It must be noted that the main source of error in the experiment was the non-axisymmetric perturbation of the free surface caused by the irregularities of the supporting rod and the consequent variations of the contact angle along the two triple contact lines. Fig. 3a shows the eccentricity, defined as $E \equiv |x_l - x_s| - |x_r - x_s|$, for the image shown in Fig. 2, where $x_l(z)$ and $x_r(z)$ are the left and right contours, respectively. There were eccentricities of about $1\ \mu\text{m}$ close to the two triple contact lines probably because wetting was not fully uniform over the rod surface (in spite of the rod having been carefully cleaned and manipulated). The eccentricity went down to values of the order of $100\ \text{nm}$ within the interval $175 < z < 450\ \mu\text{m}$. When the symmetry axis was calculated considering this interval only, the average value of $|E|$ was about $68\ \text{nm}$ (see the inset in Fig. 3a). This small non-axisymmetric perturbation of the free surface was partially removed by considering the axisymmetric contour $F = (x_l + x_r)/2$ (Fig. 3b). All the calculations were repeated for each of the ten images acquired in an experiment to obtain the average free surface contour and the standard deviations. The standard deviations were smaller than $50\ \text{nm}$, which indicates the uncertainty associated with the image processing technique. The local mean curvature was calculated from the average free surface contour using the smoothing procedure proposed in [8].

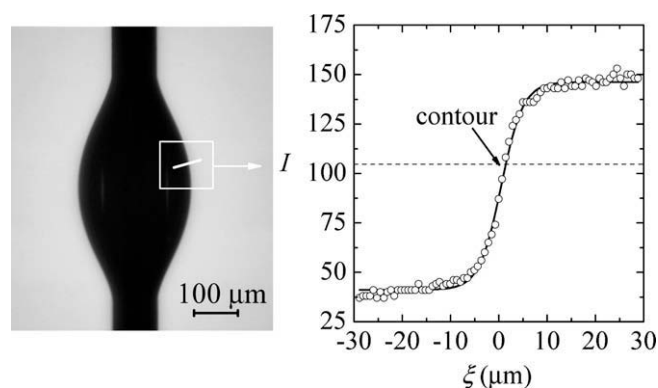


Fig. 2. Image acquired in an experiment, the gray intensity profile along the line indicated in the image (symbols), and the fitted sigmoid function (solid line).

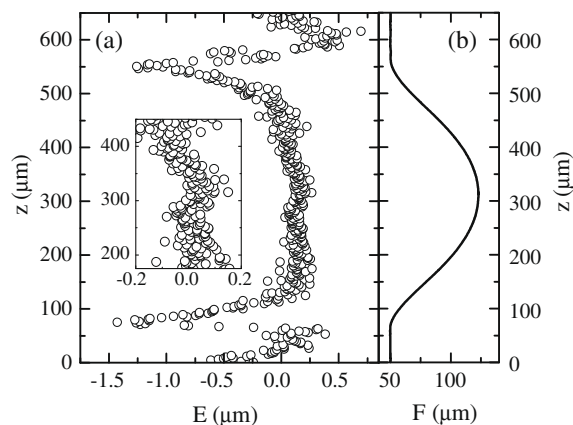


Fig. 3. Eccentricity $E(z)$ (a) and axisymmetric contour $F(z)$ (b) corresponding to the image shown in Fig. 2. The inset shows the eccentricity with respect to the symmetry axis calculated considering the interval $175 < z < 450\ \mu\text{m}$.

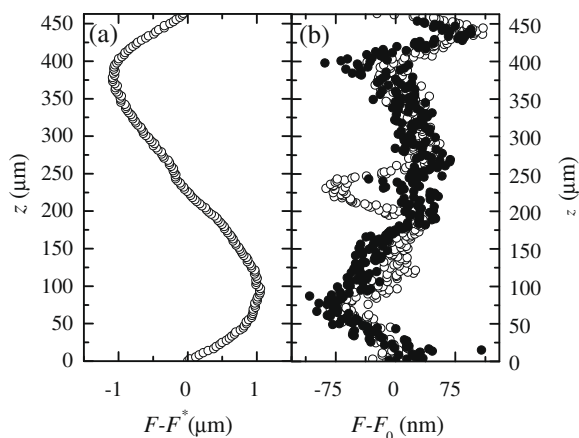


Fig. 4. Deviations of the free surface position with respect to the solutions of the Young-Laplace equation. $F^*(z)$ and $F_0(z)$ are the solutions calculated for zero Bond number and its actual value $B = 7.77 \times 10^{-4}$ in the experiment, respectively. The open symbols are the results obtained by the fitting procedure, while the dots correspond to the spline interpolation technique.

3. Results

Fig. 4 shows the deviation of the free surface position with respect to the solutions of the Young-Laplace equation $F^*(z)$ and $F_0(z)$, calculated for zero Bond number¹ and for its actual value $B = 7.77 \times 10^{-4}$ in the experiment, respectively. Those solutions were obtained by considering the volume and fixed-contact-line boundary conditions measured from the images, and the literature values of the surface tension and liquid density. It can be easily verified that, due to the very small value of the Bond number, errors smaller than 10% in the surface tension and liquid density values do not affect significantly the solution to the Young-Laplace equation [10]. The integration of the Young-Laplace equation was performed using the Runge-Kutta method, and the initial conditions and capillary pressure which lead to the boundary conditions and prescribed volume were found by the secant method. More details of the calculation can be found elsewhere [10].

The image analysis revealed the amphora-type sub-micrometer free surface deformation $F - F^*$ due to the force of gravity (Fig. 4a). The deviations with respect to the expected shape F_0 were smaller than 100 nm (Fig. 4b). One observes no clear spatial structure in $F - F_0$, which indicates that the errors must be mainly assigned to the image processing. The average value of $|F - F_0|$ in Fig. 4b was 30.7 nm, about 25 times smaller than the pixel size and 500 times smaller than the edge width. This is the main result of the present analysis, and shows the remarkable potential of optical imaging in microfluidics. The average deviation calculated from an image was 39.2 nm, which shows the positive effect of averaging over different images. The dots in Fig. 4b correspond to the results obtained by the (standard) spline interpolation technique at the sub-pixel level [8,11], instead of the fit with a sigmoid function [9]. In this case, the average deviation was 35.1 nm, which shows the slight superiority of the fitting method. Similar results were obtained in further experiments with different liquid volumes.

The precision exhibited by the optical imaging method allows one to measure the (very small) gauge pressure inside small liquid equilibrium shapes from the curvature of their free surfaces. For instance, Fig. 5 shows the pressure field inside the liquid film in Fig. 2a. The linear fit to the experimental results deviated from

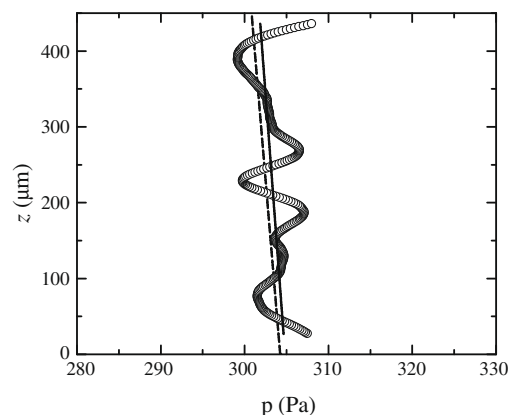


Fig. 5. Gauge pressure field inside the liquid film shown in Fig. 2a (symbols), its linear fit (solid line), and the theoretical prediction (dashed line).

the theoretical prediction calculated from $F_0(z)$ by 1 Pa. The uncertainty was smaller than 5%. The sinuous shape of $p(z)$ suggests that the uncertainty was mainly caused by the polynomial shape assumed in the smoothing procedure, rather than by the noise in the image.

The applicability of optical imaging in microfluidics is illustrated in Fig. 6. The photograph shows a water meniscus produced in a flow focusing experiment. Flow focusing uses a co-flowing stream of an immiscible phase forced through a small aperture to stretch a fluid meniscus until a thin jet is emitted from its tip [12]. In the experiment showed in the figure, a co-flowing air stream was driven by a pressure drop $\Delta P = 86$ mbar while a flow rate $Q = 160$ $\mu\text{l}/\text{min}$ of water was injected. Optical imaging allowed us to accurately measure the free surface position and its local mean curvature, which is proportional to the normal stress jump $\Delta\tau_n$ across the free surface. A smooth curve was obtained for the curvature in spite of its evaluation involves the numerical calculation of the first and second derivatives of the free surface position.

4. Concluding remarks

The validity of optical imaging for microfluidic applications has been explored in this note. The contours of liquid films at equilibrium were compared with the corresponding solutions to the Young-Laplace equation finding deviations of the order of tens of nanometers.

It must be noted that the boundary conditions and the volume used to integrate the Young-Laplace equation were affected by the errors associated with the image processing techniques. For this reason, the accuracy of the optical imaging method can not be definitively established from the comparisons presented in this note. Such validation would require the use of a theoretical solution calculated without resorting to any information coming from the tested experimental method. However, there are infinite curves that verify the boundary and volume conditions obtained in the experiment. We have shown that optical imaging “selects” among them a curve which deviates from the solution to the exact Young-Laplace equation in tens of nanometers. This result may be a significant contribution not only to fluid mechanics but also to the broader field of metrology. Indeed, equilibrium liquid shapes are excellent testbeds for object recognition techniques, because the smooth surfaces that delimit them satisfy the exact Young-Laplace equation.

It must also be noted that the image processing technique used in the present work can a priori be applied to locate the contours of any object because it does not assume the existence of a particular shape. In this sense, it differs from other image processing techniques used,

¹ The Bond number is defined as $B \equiv \Delta\rho g R_0^2 / \sigma$, where $\Delta\rho$ is the density jump across the free surface, g the gravity, R_0 the average radius of the triple contact lines, and σ the surface tension. For hexadecane, $\Delta\rho = 772$ kg/m^3 and $\sigma = 0.0262$ N/m .

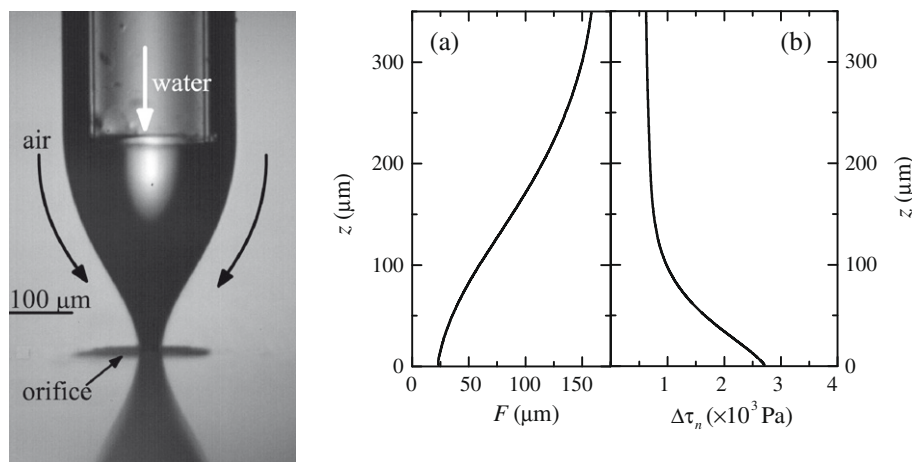


Fig. 6. (Left) Image of a water ($\rho = 998 \text{ kg/m}^3$ and $\sigma = 0.0728 \text{ N/m}$) meniscus in a coflowing air stream. (Right) Free surface position F (a) and normal stress jump $\Delta\tau_n$ across the free surface (b).

for instance, to measure the surface tension [13]. However, detecting complex contours (rough contours or with vertexes) may lead to errors significantly larger than those obtained with smooth surfaces. Verifying the accuracy of the method in those cases constitutes an interesting goal out of the scope of the present study.

There is a fundamental maximum to the resolution of any optical system which is due to diffraction. Diffraction blurs the images widening the edges of the objects up to several times the wavelength of the radiation used to illuminate them. This effect limits the minimum distance between distinguishable objects (the resolution) of an image. The resolution obtained with conventional optical lenses and visible light is of the order of several microns, and then objects separated by sub-micrometer distances overlap and can not be distinguished. Our images contain a single object (the liquid film on the rod) delimited by an edge whose width is about 10 μm (see Fig. 2), much larger than the wavelength of visible light as one could expect because of diffraction. The use of an image processing technique allows one to “get into” the region occupied by the edge to determine its true position. The discrepancy between the results obtained by this method and the true values can a priori be smaller than the wavelength of the radiation, even though the edge width is quite larger than that wavelength.

Acknowledgments

This research was supported by the Ministerio de Educación y Ciencia (Spain) through Grant No. DPI2007-63559. Partial support from the Junta de Extremadura through Grant No. GRU07003 is also acknowledged.

References

- [1] O.A. Basaran, *AIChE J.* 48 (2002) 1842.
- [2] R. Suryo, O.A. Basaran, *Phys. Fluids* 18 (2006) 082102.
- [3] A. Barrero, I. Loscertales, *Annu. Rev. Fluid Mech.* 39 (2007) 89.
- [4] J. Fernández de la Mora, *Annu. Rev. Fluid Mech.* 39 (2007) 217.
- [5] R.T. Collins, J.J. Jones, M.T. Harris, O.A. Basaran, *Nat. Phys.* 4 (2008) 149.
- [6] S.T. Thoroddsen, T.G. Etoh, K. Takehara, *Annu. Rev. Fluid Mech.* 40 (2008) 257.
- [7] R. Sattler, C. Wagner, J. Eggers, *Phys. Rev. Lett.* 100 (2008) 164502.
- [8] J.M. Montanero, C. Ferrera, V.M. Shevtsova, *Exp. Fluids* 45 (2008) 1087.
- [9] B. Song, J. Springer, *J. Colloid Interface Sci.* 184 (1996) 77.
- [10] J.M. Montanero, M.G. Cabezas, F.J. Acero, J.M. Perales, *Phys. Fluids* 14 (2002) 682.
- [11] H. Tavana, A.W. Neumann, *Adv. Colloid Interface Sci.* 132 (2007) 1.
- [12] A.M. Gañán-Calvo, *Phys. Rev. E: Stat., Nonlinear, Soft Matter Phys.* 78 (2008) 026304.
- [13] M.G. Cabezas, A. Bateni, J.M. Montanero, A.W. Neumann, *Langmuir* 22 (2006) 10053.